Practical Contour Tracing Via Integration of Adaptive Contrast Stretching and Gabor Wavelet Transform

Zhengmao Ye, Habib Mohamadian, Hang Yin, Yongmao Ye

Abstract—The Gabor filter is applied using discrete wavelet transform for edge detection and contour tracing on true color images, whose wavelet functions provide the high resolution in both spatial and frequency domains. The number of wavelets also affects the quality of edge detection. To generate more accurate outcomes, integration of adaptive contrast stretching and Gabor wavelet transform is properly carried out for edge detection and contour tracing on broadly selected images. Contrast stretching is based on adaptive histogram equalization generalization, where the accumulation function is used to generate intensity mapping of three primary color components stem from local histograms. Any digital image consists of major objects, edges, corners and blobs as well as the noises and background fluorescence. Critical changes in image properties can be captured via detecting sharp variations in the intensity. Although the gray level intensity is commonly used for edge detection, the mixture of true color components (red, green, and blue) gives rise to an overall appeal with better visual effect and color balance by rendering three specific colors. In fact, edges, contours and boundaries could be detected in various ways by means of intensity changes, however, edge broken and false detection are among typical drawbacks in classical approaches, which are subject to information loss and feature deformity. The popular Canny edge detection (CED) and Ant Colony Optimization (ACO) detection are among the most effective approaches for edge detection and contour tracing. With the benefit of artificial intelligence, the performance of ACO can be slightly better than CED, however, the tradeoff is the much larger computation complexity. Instead, Gabor wavelet detection offers similar computation cost to CED, but dramatically better outcomes are produced with relatively less efforts. A comparison between Canny edge and Gabor wavelet detection is also made in terms of both visual appealing and quantitative evaluation.

Keywords—Gabor Wavelet Transform, Adaptive Contrast Stretching, Canny Edge Detection, Quantitative Analysis

I. Introduction

The energy distribution of a light source depends not only on the image coordinate (x, y, z) but also on the time and wavelength. Each entry of an image matrix is corresponding to the brightness or darkness at that pixel.

Zhengmao Ye, Habib Mohamadian, Hang Yin
College of Engineering, Southern University
Baton Rouge, Louisiana 70813, USA

Yongmao Ye
Broadcasting Department, Liaoning TV Station
Shenyang, 110000, China

Edge detection is the fundamental technique to identity sharp intensity changes and feature discontinuities, due to illumination fluctuation, surface orientation, background fluorescence and material property. The ideal edge detector should generate a set of connected curves that represent boundaries of objects and markings, as well as discontinuities in surface orientation [1-3]. Search-based and zero-crossing based algorithms are two major edge detection approaches. The search-based methods seek for the local directional optima of the 1st order gradient magnitude to detect edge strength. Zero-crossing based methods compute zero crossings in the 2nd-order Laplacian of Gaussian filter to capture edges. The discontinuous fragments and false edges always occur accordingly. Classical approaches involve specific templates or smoothing functions, like Sobel and Prewitt methods, which are also susceptible to broken edges and information loss. It could be tough to connect edges accurately even with the compensation techniques. This leads to implementations of famous Canny edge detection and ACO detection algorithms. The Canny method searches for edges at the local optima of intensity gradients using a Gaussian filter, while a chain code is necessary because CED has difficulty in connecting the broken edges. As two thresholds are introduced to detect the strong and weak edges, false detection of noisy information may occur easily. The enhanced ACO scheme is implemented whose optimal solutions are then used as initial control points. It is subject to further adaptive contour tracking. Thus the M-connectivity is applied to maintain a desired number of the connected pixels [3-5]. ACO could produce better edge detection at an extra expense, however. Now an effective but simple approach is pending.

Gabor wavelets are well suitable for object representation. Although 2D Gabor is not orthonormal wavelet transform, it can provide complete representation under some specified conditions, which can be applied to various image processing issues and further extended to real world problems like vehicle verification [6-7]. In order to expand Gabor edge detection to open contour tracing and closed boundary tracking without the need of additional M-connectivity chain code, fragmentation due to weak contrast or strong threshold should be minimized. Adaptive image contrast enhancement could be implemented which covers histogram equalization generalization. By virtue of parameter adjustment, adaptive contrast stretching has shown multiple degrees of contrast enhancement, yielding complete adaptive equalization at an extreme [8-10]. Thus integration of Gabor wavelet transform and adaptive contrast stretching based on histogram equalization is proposed for simultaneous edge detection and contour tracing. It will be applied to a set of true color images with edges and contours represented by all three color components, making sharp edge contours with optimal color fidelity and visual appeals. The merits of integration can be easily observed from visual effects

on broad collection of diverse examples. The quantitative metrics can be further used to evaluate the impact of proposed technology integration on edge detection and contour tracing over the well-recognized classical approaches [11-12].

II. Adaptive Contrast Stretching

A. *Digital Image True Color Model*

The true color system contains three additive primary colors (red, green, and blue), where each color represents a primary spectral component in the Cartesian coordinate system. Each pixel in a digital image has its own bit-depth value, where the grayscale image supports 8-bit and true color image supports 24-bit. In true color subspace, each color is uniquely mapped into a cube where red, green, and blue are placed on three corners. Black locates at the origin and white locates at the corner opposite to black. Three other colors (cyan, magenta, yellow) are placed on three opposite corners. The least value zero is corresponding to color of black and highest value one is corresponding to color of white. The grey scale lies along with main diagonal that links black and white corners. Each color, shade, and hue acts as a vector on or inside the cube pointed from the origin. The visual display depends on the actual combination of red, green, and blue in either unequal or equal intensities (grayscale). The color intensity component comes from additive color mixing out of three primary coordinates. Image quantization acts as the A/D transition between the continuous image and its digital integer equivalent. Linearity is assumed such that three primary color intensity components in the RGB system are independently processed before arbitrary composition true color is reached.

B. *Histogram Equalization and Adaptive Contrast Stretching*

Contrast stretching is to enlarge the dynamic range of digital images where sharpening is a standard technique. Contrast is enhanced locally instead of globally. More visible artifacts are sensed and displayed via contrast enhancement against the limitation of sensing when low contrast images are captured under poor illumination with the limited dynamic range. Adaptive neighborhood is set up for each seed pixel which applies uniform distribution for contrast transformation. All neighboring pixels involve in contrast transformation. It is feasible to enhance contrast across the region rather than at borders exclusively, so as to cover objects of interests across the neighborhood. Contrast stretching can be mapped into a specified modification curve. The visual perception under a distinguishable degree of color variations depends on the levels of contrast from true color or gray level representation. Highlights and shadows simply depict high dissimilarity of density in image tones for the high contrast images. At the same time, low contrast images are corresponding to less dissimilarity of density in image tones. The root mean square contrast τ is defined as the standard deviation of entire image pixel intensities, which is independent of spatial distribution of the pixel intensity. It is shown in (1).

$$\tau = \sum_{i=0}^{M-1} \sum_{j=0}^{N-1} \frac{[g(i,j) - g_{AVG}]^2}{M*N} \tag{1}$$

where $g(i, j)$ denotes a pixel intensity at coordinates i and j for any 2D digital image of the size $M \times N$. g_{AVG} indicates the average intensity throughout all pixels across a digital image.

The contrast-limited adaptive histogram algorithm is only applied to small regions rather than the entire digital image. Within each region, interpolation is necessary so as to estimate the brightness of pixels not available. Bilinear interpolation is applied which has the merit of exerting small decrement in resolution to avoid randomly induced artifacts and boundaries. Adaptive contrast enhancement in terms of the histogram equalization is implemented. Similar to contrast stretching of gray level images, each of three primary color components is processed separately using the adaptive histogram equalization algorithms. In contrast stretching, the adaptive neighborhoods of the foreground and background are constructed, where the background size and foreground size are comparable to each other. The constraint is introduced to the contrast inside the homogeneous areas to avoid amplifying noises. A true color image is split into a number of small regions. Within each region, histogram is computed with the contrast constraint, and then exponential distribution is estimated as a basis to create the contrast transform function. Mapping from local histogram is generated by specifying the assignment of pixels in each small local region. Around the selected seed pixel's neighborhood, adaptive contrast stretching is conducted until satisfactory contrast is achieved. The intensity is shown in (2).

$$I_{out}(i, j) = \mu \frac{I_{in}(i, j) - Min(i, j)}{Max(i, j) - Min(i, j)} \tag{2}$$

where $I_{in}(i, j)$ is the brightness intensity value of the measured seed pixel, μ is the contrast limitation factor that is chosen to produce the desired dynamic range and also to prevent over saturation of the image in homogeneous areas. Max and Min are maximal and minimal values around the seed pixel neighborhood, $I_{out}(i, j)$ is the enhanced intensity value after contrast stretching. The optimal number of small data regions depends on the size of source images. Excessive enhancement of noises is avoided when using the adaptive schemes since an evenly distributed smooth contrast stretching is generated across the entire region via bilinear interpolation. Excessive enhancement of contrast is also avoided by upper and lower level parameter constraint against saturation. The histogram of each color component (red, green and blue) contains 256 bins. The percentage of counts for each color bin over the total accumulation gives rise to the probability distribution. Tuning is made adaptively on the exponential function parameters, contrast limiting factors and bilinear interpolation weights in order to reach high quality contrast stretching. The outcomes of adaptive contrast stretching will be used as the input images to 2D Gabor wavelet transform for edge detection and contour tracing, covering patterns in terms of all three primary color components. Furthermore, comparisons with the classical edge detection approach will also be made.

III. Gabor Transform for Edge Detection and Contour Tracing

The 2D Gabor function h(x,y) is formulated as a Gaussian kernel function modulated by a sinusoidal plane wave. In the spatial domain, a 2D Gabor filter is the product of an elliptical Gaussian and a complex sinusoid. Let s(x,y) be a complex sinusoid carrier and g(x,y) be a 2D Gaussian shaped envelope, then h(x,y), s(x,y) and g(x,y) are formulated as (3-5), where σ_x and σ_y are the standard deviations in x and y axes, u_0 and v_0 are the spatial central frequency of the 2D Gabor function.

$$h(x,y)=s(x,y)g(x,y) \tag{3}$$

$$s(x, y)=e^{-j2\pi(u_0x+v_0y)} \tag{4}$$

$$g(x, y)=\frac{1}{2\pi\sigma_x\sigma_y}e^{-(\frac{x^2}{2\sigma_x^2}+\frac{y^2}{2\sigma_y^2})} \tag{5}$$

The 2-D Gabor filter is thus expressed as:

$$h(x, y)=s(x, y)g(x, y)=\frac{1}{2\pi\sigma_x\sigma_y}e^{-(\frac{x^2}{2\sigma_x^2}+\frac{y^2}{2\sigma_y^2})}e^{-j2\pi(u_0x+v_0y)} \tag{6}$$

In the frequency domain, the frequency response of the 2D Gabor function is shown in (7) with the frequency shifts along the u axis and v axis.

$$H(u, v) = G(u-u_0, v-v_0) \tag{7}$$

Using convolution theorem, H(u, v) is formulated as (8):

$$H(u, v)=\frac{e^{-[\frac{(u-u_0)^2}{2\sigma_u^2}+\frac{(v-v_0)^2}{2\sigma_v^2}]}}{2\pi\sigma_x\sigma_y}=2\pi\sigma_u\sigma_ve^{-2\pi^2[(u-u_0)^2\sigma_u^2+(v-v_0)^2\sigma_v^2]} \tag{8}$$

where σ_u and σ_v are the standard deviations in u and v axes,

$$\sigma_u=\frac{\sigma_x}{2\pi}; \sigma_v=\frac{\sigma_y}{2\pi} \tag{9}$$

The 2D Gabor wavelets are generated by two operations of rotation and dilation with respect to the Gabor function.

$$g_{mn}(x, y) = g(x', y')/ \alpha^m \tag{10}$$

where the scaling factor s = $\alpha^{(-m)}$ ($\alpha>1$ and m = 0, 1, ..., M−1) and the phase factor θ_n = $n\pi$ /N (n = 0, 1, ..., N−1). M and N indicate the total number of scales and orientations. After rotation, (x', y') is formulated as (11), which can also be expressed as (12).

$$\begin{bmatrix} x' \\ y' \end{bmatrix}=\begin{bmatrix} \cos\theta_n & \sin\theta_n \\ -\sin\theta_n & \cos\theta_n \end{bmatrix}\begin{bmatrix} x \\ y \end{bmatrix} \tag{11}$$

$$x'= x \cos\theta_n+ y \sin\theta_n \text{ and } y'= - x \sin\theta_n+ y \cos\theta_n \tag{12}$$

Gabor wavelets are symmetric thus the value of θ_n is specified to realize an evenly sampled space within [0, π]. 16 Gabor wavelets are generated The Gabor filter consists of both the real and imaginary components, where two components are orthogonal to each other. Integration of adaptive contrast stretching and 2D Gabor wavelet transform is proposed for edge detection and contour tracing, without the presence of fragment linking in terms of the M-connectivity chain code. Technology integration of adaptive contrast stretching and discrete 2D Gabor wavelet transform is implemented next.
.

IV. Case Studies of Typical Images

In Figures 1 and 2, 12 well-known landmark images and 3 monument architecture images are selected for experiments. Without loss of generality, instead of choosing some standard testing images in fields of pattern recognition and image processing, selected digital images for numerical simulations include pictures taken from several continents of Asia, Africa, (North, Central, South) America, Europe, and Oceania. First of all, adaptive contrast stretching and discrete 2D Gabor wavelet transform are applied to all three primary color components separately. Gabor wavelets being generated will be combined next so that edges and contours for each primary color component can be collected. Additive color mixing at each image pixel is then conducted so that composite edges and contours in the true color format are produced. Finally, the outcomes of edge detection and contour tracing are compared with the popular conventional edge detection approach.
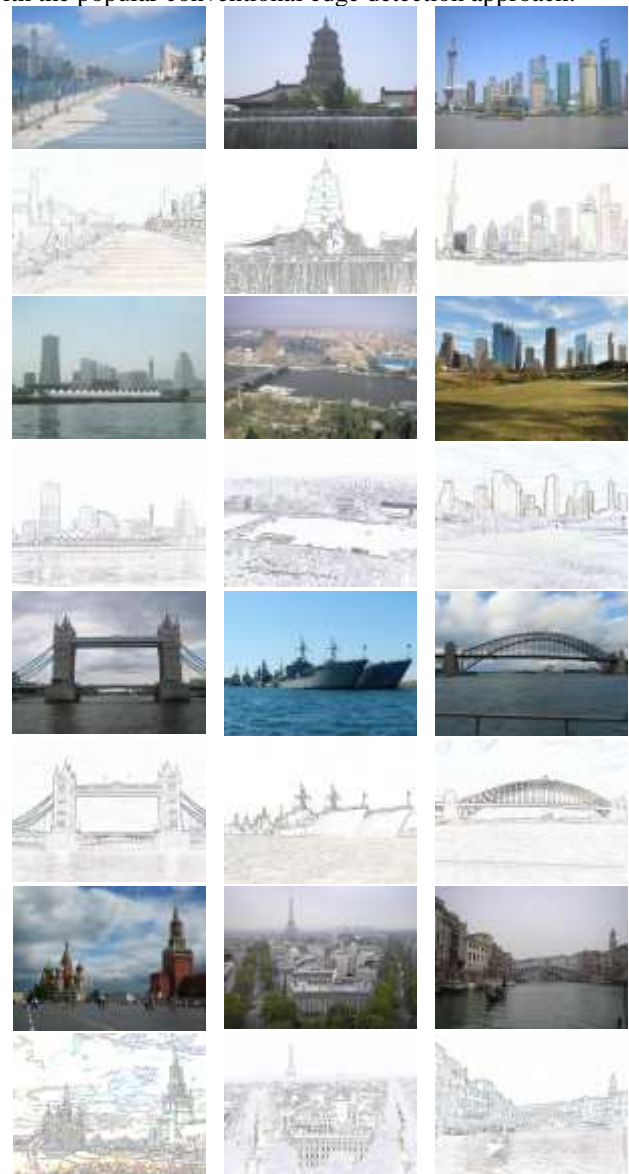

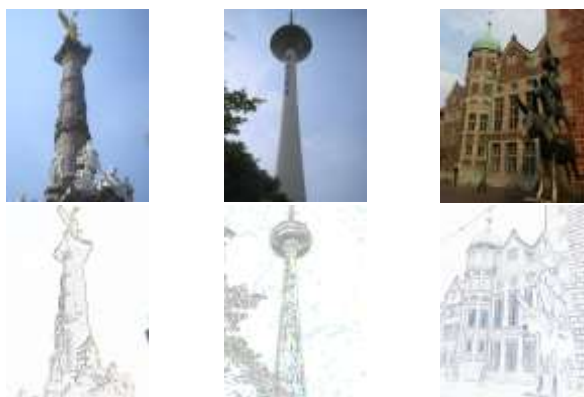Figure. 1 Source Images and Contour Images of Landmarks

Figure. 2 Source Images and Contour Images of Monuments

V. Comparisons of Gabor Wavelet and Canny Edge Detection

The integration approach using adaptive contrast stretching and 2D Gabor wavelet transform has provided satisfactory outcomes in diverse testing cases from the visual appeals. No post processing technique is applied above at all to link gaps between edges and to represent contours and boundaries. As a matter of fact, numerous conventional approaches have been designed for edge detection. In a long list of classical methods, Canny edge detection is broadly accepted as the best one, so Canny edge detection is used as a reference to evaluate the proposed approach. The Canny edge scheme detects edges at zero-crossings of the second order directional derivative of the digital images. The Canny operator is applied step by step which uses an optimal Gaussian smoothing filter in (13).

$$G(x, y, \sigma) = \frac{1}{2\pi\sigma^2} \exp(-\frac{x^2 + y^2}{2\pi\sigma^2}) \qquad (13)$$

The digital image is smoothed by Gaussian convolution.

$$H(x, y) = G(x, y) * I(x, y) \qquad (14)$$

where $G(x, y)$ is the Gaussian smoothing filter; $I(x, y)$ is the intensity of the source image, $H(x, y)$ is the intensity of the smoothed image and * denotes convolution operation. The first order derivative is applied to compute both the magnitude and direction of the gradient. The local optima of the first order derivative of $H(x, y)$ is calculated in the direction n for locating edges, which is corresponding to the zero-crossing point of the second order derivative of $H(x, y)$ as shown in (15). The edge direction will be rounded to one of eight phase angles in order to represent vertical, horizontal and diagonal directions. Non-maximal suppression is then applied to the gradient. As a result, edge points whose gradient magnitude (strength) reaches a local maximum are located.

$$\frac{d^2(G*I)}{dn^2} = \frac{d(\frac{dG}{dn}*I)}{dn} = 0 \qquad (15)$$

Figure. 3 Comparison of Detection Images by Canny and Gabor Detection

In (15), n represents the direction of the gradient magnitude of the digital image. Each pixel's edge gradient is computed and compared with gradients of all the 8 neighbors along the gradient direction. To sketch the curve for a contour and the regional boundary, the next step is edge linking so that broken edges and line segments in the neighborhood are connected. Fragmentation means a spurious loss of edge points, which destroys the connectivity of the edge. The chain code criterion is introduced which is applied to each visiting node. The chain code involves a digital curve being represented by an integer sequence based on the relative orientation of the edge pixel to neighbors at the 2D spatial domain. The 8-connectivity chain code is applied to all the immediate pixels surrounding the testing pixel. This is the way to depict the pixel thin curve trajectory. To apply the thin chain code, start from one pixel endpoint, evaluate in the counter-clockwise direction on the next searching pixel, and encode the pixel until stagnation occurs or the maximum number of cycles is reached. Canny edge detection has the potential of solid edge tracing, clear marking and appropriate localization, since thresholding with hysteresis (with high threshold and low threshold) will be used together. The high threshold is applied to locate true edges as starting endpoints initially. However, a high threshold may cause important information missing such as the subtle and discontinuous edges. If no starting point is captured, the algorithm lowers the high threshold so as to make sure that starting points will be detected. Directional information is then introduced so that edges can be traced throughout the entire images. The low threshold definitely helps to detect more edges, but noisy and irrelevant information could be detected as well, possibly resulting in false edges and poor localization. In fact, a smoothing Gaussian filter for Canny edge algorithms partially compensate for this effect.

In Figure 3, two sets of testing results are shown. The results from Gabor detection are shown to the left and those from Canny detection are shown to the right. When the comparison is made between Gabor detection and Canny edge detection plus chain code tracking, better visual observation is made using Gabor detection. The individual edges, region contours and boundaries using 2D Gabor filter are clearly shown. Phenomena of curve fragmentation and false detection appear frequently at Canny edge detection with ambiguous contours and boundaries. It results from noisy information and trivial artifacts. Meanwhile, to quantitatively evaluate two sets of results based on Gabor detection and Canny detection, two metrics of correlation and homogeneity are introduced.

Correlation acts as a standard measure to interpret linear dependency of the color intensity levels among neighboring pixels. It depicts the actual amount of local variations across a digital image. The correlation ρ is formulated as (16).

$$\rho = \sum_{i=0}^{M-1}\sum_{j=0}^{N-1} \frac{(i-\mu_i)(j-\mu_j)}{\sigma_i \sigma_j} g(i,j) \qquad (16)$$

$$\sigma_i = \sum_{i=0}^{M-1}\sum_{j=0}^{N-1}(i-\mu_i)^2 g(i,j); \mu_i = \sum_{i=0}^{M-1}\sum_{j=0}^{N-1}[i*g(i,j)] \text{ (for i or j)}$$

where M and N represent total numbers of pixels in the row and column of the digital image; i and j represent the x and y coordinates of the co-occurrence matrix; g(i, j) is the pixel intensity in the co-occurrence matrix at coordinates i and j. μ_i and σ_i are the horizontal mean and variance, and μ_j and σ_j are the vertical mean and variance. σ_i and σ_j are metrics of the tone variance of each primary color component.

Homogeneity acts as another measure of the local intensity distribution of the true color or gray level images. Higher homogeneity measure values indicate less structural variations and lower ones indicate more structural variations instead. The homogeneity Φ is formulated as (17).

$$\Phi = \sum_{i=0}^{M-1} \sum_{j=0}^{N-1} \frac{1}{1+(i-j)^2} g(i,j) \tag{17}$$

where M and N represent total numbers of pixels in the row and column of the digital image; i and j represent the x and y coordinates of the co-occurrence matrix; g(i, j) is the pixel intensity in the co-occurrence matrix at coordinates i and j.

TABLE I.   IMAGE METRICS BY CANNY AND GABOR DETECTION

Case 1	Red	Green	Blue
Correlation **Gabor**	**0.8794**	**0.8669**	**0.8346**
Homogeneity **Gabor**	**0.9308**	**0.9338**	**0.9407**
Correlation **Canny**	0.4233	0.4110	0.4222
Homogeneity **Canny**	0.8509	0.8695	0.8540
Case 2	Red	Green	Blue
Correlation **Gabor**	**0.8870**	**0.8904**	**0.8957**
Homogeneity **Gabor**	**0.9738**	**0.9729**	**0.9718**
Correlation **Canny**	0.3251	0.3146	0.3320
Homogeneity **Canny**	0.9130	0.9173	0.9096

For both Case 1 and Case 2 in Table 1, correlations of three primary color components in detection images from Gabor wavelet transform are much larger than those from Canny detection. It shows that Gabor detection does capture sharper edges with the higher intensity contrast when compared with Canny detection. For each primary color component, more intrinsic information has been discovered by Gabor detection. Similarly, for both cases, homogeneities of three primary color components in detection images from 2D Gabor wavelet transform are greater than those from Canny detection. It shows that 2D Gabor wavelet transform is less sensitive to the noisy information whose false detection rate is actually much lower than that of Canny detection. Based on the quantitative metrics, technology integration of adaptive contrast stretching and 2D Gabor wavelet transform does give rise to high quality edge detection and contour tracing.

VI. **Conclusions**

The 2D Gabor wavelet transform has been introduced in this work. Edge detection and contour tracing are conducted by convolution of each of three primary color components of digital images with the 2D Gabor wavelet in the frequency domain. Integration of adaptive contrast stretching and Gabor edge detection results in better quality edge detection and contour tracing with sharper patterns. The visual effect of the proposed simple approach is testified by a set of digital images collected from 6 continents. Perfect connectivity of edges and corners is observed using Gabor wavelet detection. Rather than regular gray level edge detection, color balance is also taken into account by mixing intensities of primary red, green, and blue color components, so that detail contour information and visual appearance are achieved. The actual contour tracing outcomes outperform those from combination of widely adopted Canny edge detection and M-connectivity chain code, which indicates that simple Gabor wavelet detection is indeed more successful without loss of critical edges and feature deformity. In this case, sharp intrinsic edge and contour information has been extracted without the necessity of suffering from the excessive computation expense.

References

[1] R. Gonzalez and R. Woods, "Digital Image Processing," 2nd Edition, Prentice-Hall, 2002

[2] A. Shapiro, G. Stockman, C. George, "Computer Vision". Prentice Hall, ISBN 0-13-030796-3, 2002

[3] Z. Ye, H. Mohamadian and Y. Ye, "Quantitative Analysis of Feature Detection Using Adaptive Canny Edge Detector and Enhanced Ant Colony Optimization", International Journal of Modeling and Optimization, pp. 210-215, Vol. 2, No. 4, 2012, ISSN: 2010-3697

[4] Z. Ye, H. Mohamadian, "Strengthen Accuracy of Feature Recognition via Integration of Ant Colony Detection and Adaptive Contour Tracking", Proceedings of the 2011 IEEE Congress on Evolutionary Computation, pp. 1799-1804, June 5-8, 2011, New Orleans, USA

[5] A. Baterina and C. Oppus, "Image Edge Detection Using Ant Colony Optimization", International Journal of Circuit, Systems and Signal Processing, pp.26-33, Issue 2, Vol 4, 2010

[6] T. Lee, "Image Representation Using 2D Gabor Wavelets" IEEE Trans on Pattern Analysis and Machine Intelligence, Vol. 18, No. 10, 1996

[7] J. Arrospide, L. Salgado, "Log-Gabor Filters for Image-Based Vehicle Verification", IEEE Transactions on Image Processing, Vol. 22, No. 6, pp. 2286-95, June 2013

[8] J. Stark, "Adaptive Image Contrast Enhancement Using Generalizations of Histogram Equalization", IEEE Transactions on Image Processing, pp. 889-896, Vol. 9, No. 5, May 2000

[9] Z. Ye and H. Mohamadian, "Underwater Scene Characterization Using Wavelet Packet Denoising and Adaptive Contrast Stretching", Proceedings of the 2012 International Symposium on Signals, Systems and Electronics, pp. 349-354, October 03-05, 2012, Potsdam, Germany

[10] G. Papari and G. Petkov, "Edge and Line Oriented Contour Detection: State of the Art", Image and Vision Computing, v 29, n 2-3, 79-103, Feb 2011, Elsevier Science

[11] Z. Ye, H. Mohamadian and Y. Ye, "Information Loss Determination on Digital Image Compression and Reconstruction Using Qualitative and Quantitative Analysis", Journal of Multimedia, ISSN: 17962048, Academy Publisher, Vol. 6, No. 6, pp. 486-493, December, 2011

[12] Z. Ye, H. Cao, S. Iyengar and H. Mohamadian, "Medical and Biometric System Identification for Pattern Recognition and Data Fusion with Quantitative Measuring", Chapter 6, Systems Engineering Approach to Medical Automation, Artech House Publishers, pp. 91-112, Sept 2008